CANCER BIOLOGY & THERAPY
2016, VOL. 17, NO. 11, 1158–1167
http://dx.doi.org/10.1080/15384047.2016.1235663

Taylor & Francis
Taylor & Francis Group

RESEARCH PAPER

OPEN ACCESS

Novel anti-EPHA2 antibody, DS-8895a for cancer treatment

Jun Hasegawa[a], Mayumi Sue[a], Michiko Yamato[a], Junya Ichikawa[a], Saori Ishida[a], Tomoko Shibutani[b], Michiko Kitamura[a], Teiji Wada[a], and Toshinori Agatsuma[a]

[a]Biologics & Immuno-Oncology Laboratories, Daiichi Sankyo Co., Ltd., Shinagawa-ku, Tokyo, Japan; [b]Translational Medicine & Clinical Pharmacology Department, Daiichi Sankyo Co., Ltd., Shinagawa-ku, Tokyo, Japan

ABSTRACT

Overexpression of EPHA2 has been observed in multiple cancers and reported to be associated with poor prognosis. Here, we produced an afucosylated humanized anti-EPHA2 monoclonal antibody (mAb), DS-8895a for cancer treatment. The antibody recognizes the extracellular juxtamembrane region of EPHA2 and therefore can bind to both full-length and truncated forms of EPHA2, which are anchored to cell membranes and recently reported to be produced by post-translational cleavage in tumors. DS-8895a exhibited markedly increased antibody dependent cellular cytotoxicity (ADCC) *in vitro* and also inhibited tumor growth in EPHA2-positive human breast cancer MDA-MB-231 and human gastric cancer SNU-16 xenograft mouse models. Moreover, DS-8895a in combination with cisplatin (CDDP) showed better efficacy than each of the monotherapies did in the human gastric cancer model. These results suggest that a novel antibody, DS-8895a has therapeutic potential against EPHA2-expressing tumors.

Abbreviations: ADCC, Antibody-dependent cellular cytotoxicity; NK cells, Natural killer cells; mAb, Monoclonal antibody; PBMCs, Peripheral blood mononuclear cells; MT1-MMP, Membrane type-1 matrix metalloproteinase

ARTICLE HISTORY
Received 20 April 2016
Revised 8 August 2016
Accepted 4 September 2016

KEYWORDS
Afucosylated antibody; antibody-dependent cellular cytotoxicity (ADCC); cancer; DS-8895a; EPHA2; Monoclonal antibody (mAb); natural killer (NK) cells

Introduction

EPHA2 is a type-I transmembrane receptor tyrosine kinase that belongs to the EPH receptor family, and its ligands are ephrin-A1 to A5.[1] EPHA2 overexpression has been observed in a wide variety of neoplasms such as gastric cancer, colorectal cancer, esophageal cancer, non-small cell lung cancer, breast cancer, hepatocellular carcinoma, prostate cancer, ovarian cancer, pancreatic cancer, bladder cancer, cervical cancer, endometrial cancer, renal cancer, brain tumors, head and neck cancer, and melanoma.[2-18] EPHA2 is also associated with poor prognosis in cancers of the stomach, esophagus, lung, liver, ovary, endometrium, kidney, brain, and head and neck.[2,4-6,8,10,14-17] EPHA2 expression is upregulated by the Ras-extracellular signal-regulated kinase (ERK) signaling pathway, which promotes tumor growth and survival and is frequently activated by constitutive active mutations in molecules involved in the pathway or by constitutive signals from overexpressed growth factor receptors in aggressive tumors.[19,20]

Recently, it has been reported that membrane type-1 matrix metalloproteinase (MT1-MMP) on tumor cells cleaves EPHA2 at the extracellular domain and the resultant truncated and membrane-anchoring forms of EPHA2 promote oncogenic signaling.[21,22] These findings suggest that tumor cells contain not only full-length but also truncated forms of EPHA2 on their cell surface, and the truncated forms of EPHA2 are important for EPHA2-targeting cancer therapy.

In the past 2 decades, several monoclonal antibodies (mAbs) that mediate antibody-dependent cellular cytotoxicity (ADCC) have been approved for cancer treatment, including conventional antibodies: rituximab (anti-CD20 mAb), trastuzumab (anti-ERBB2 mAb), and cetuximab (anti-EGFR mAb); and glycoengineered antibodies: mogamulizumab (afucosylated anti-CCR4 mAb) and obinutuzumab (afucosylated anti-CD20 mAb).[23-26] ADCC is triggered by formation of the complex comprising antibody, its cell surface antigen on target cells, and the Fc gamma receptors (FcγRs) mainly expressed on natural killer (NK) cells and monocytes/macrophages, and leads to cell death via perforin/granzyme, TRAIL, and FasL.[27,28] These ADCC processes are also suggested to affect adaptive tumor immunity by enhancing antigen presentation.[29,30] Therefore, enhancement of ADCC is expected to be important in altering the tumor microenvironment. Afucosylation of the carbohydrate chain in human Fc has been reported to greatly enhance ADCC by increasing the binding affinity between Fc and FcγRIIIa.[31,32]

DS-8895a is a novel humanized anti-EPHA2 mAb that is afucosylated to enhance ADCC. Here, we describe the characteristics and pharmacological activities of DS-8895a.

Results

Characterization of DS-8895a

Anti-EPHA2 mAb was obtained by immunization of mice with recombinant human EPHA2 and was then humanized as

CONTACT Jun Hasegawa hasegawa.jun.hs@daiichisankyo.co.jp Biologics & Immuno-Oncology Laboratories, Daiichi Sankyo, Co., Ltd., 1-2-58 Hiromachi, Shinagawa-ku, Tokyo 140-8710 Japan.

human IgG1 to generate DS-8895a. Its binding to EPHA2 was confirmed by flow cytometric analysis using CT26.WT cells transiently transfected with wild-type or truncated mutants of human EPHA2 (Fig 1A). Wild-type EPHA2 (amino acids 24–976) was recognized by the anti-EPHA2 mAb. In contrast, the truncated mutant that lacked amino acids 438–527 did not bind to the anti-EPHA2 mAb (Fig 1B), suggesting the importance of the C-terminal fibronectin type III (FnIII) domain of EPHA2 for the binding of DS-8895a. Recently, it is reported that MT1-MMP cleaves EPHA2 at around the N-terminal FnIII domain and produces fragments comprising extracellular soluble forms and the membrane-anchored forms whose N-terminal amino acid sequence begins with Y^{385}, T^{395}, V^{432}, or N^{435} (Fig 1A).[21,22] DS-8895a bound to EPHA2ΔEN, the shortest form of truncated EPHA2 (Fig 1B), suggesting that DS-8895a detects the juxtamembrane domain of EPHA2 and binds to both full-length and MT1-MMP cleaved, namely cancer-associated forms of EPHA2.

A Blast search against human proteins identified ones similar to the region containing the C-terminal FnIII domain of EPHA2. However, DS-8895a did not bind to those proteins (Fig. 2). This result suggests that DS-8895a specifically binds to human EPHA2.

To examine the effects of DS-8895a on tyrosine phosphorylation of EPHA2, EPHA2-positive cancer cells (human triple negative breast cancer MDA-MB-231 cells and human gastric cancer 44As3 cells) were treated with DS-8895a in the presence and absence of an EPHA2 ligand, ephrin-A1. In the absence of ephrin-A1, DS-8895a treatment did not induce tyrosine phosphorylation of EPHA2 in both cell lines. In the presence of ephrin-A1, tyrosine phosphorylation of EPHA2 was observed in both cell lines, and DS-8895a partially inhibited the tyrosine phosphorylation at the highest concentration of 10 μg/mL (Fig. 3A and 3B). These results suggest that DS-8895a does not have EPHA2 agonistic activity, and has antagonistic activity.

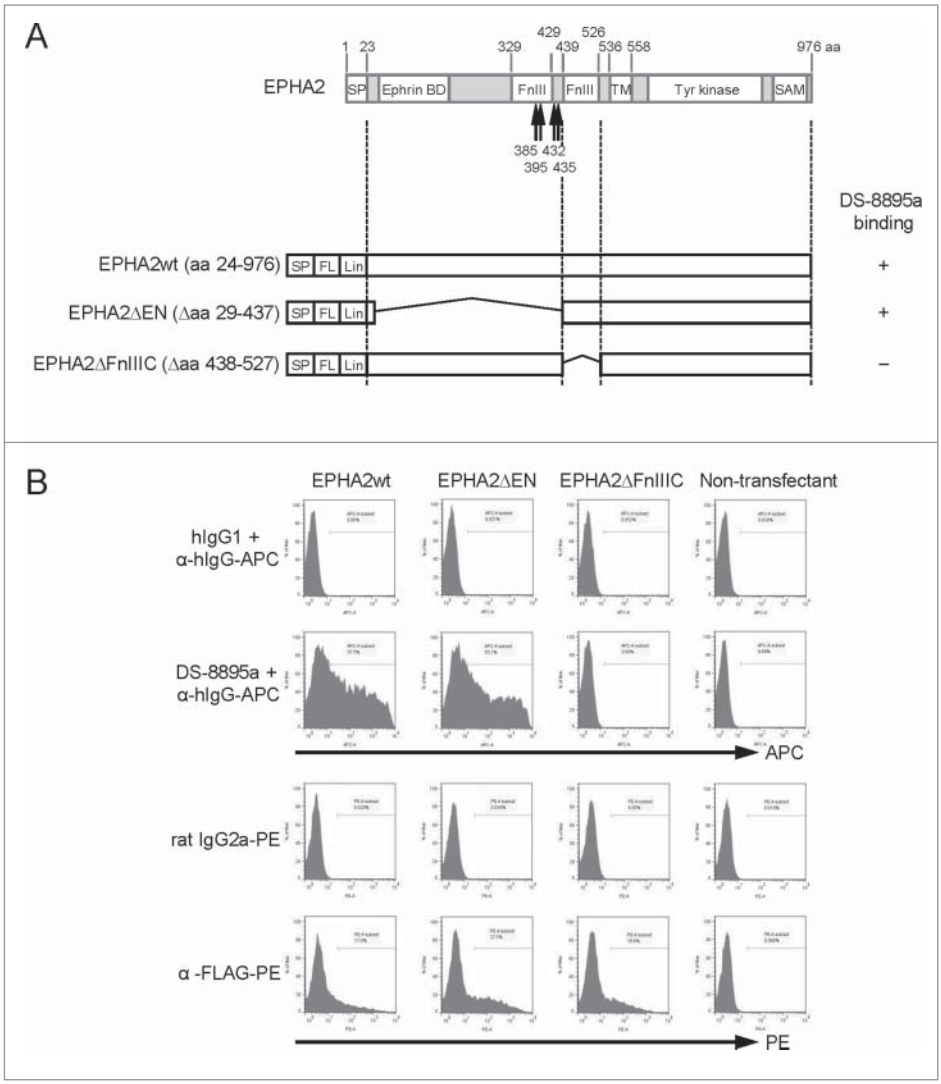

Figure 1. DS-8895a binding to wild-type and truncated mutant EPHA2 proteins. (A) Schematic representations of EPHA2 and the expression constructs used in this study. The arrows indicate sites of cleavage of EPHA2 by MT1-MMP. SP, signal peptide; FnIII, fibronectin type III domain; TM, transmembrane domain; Tyr kinase, tyrosine kinase domain; SAM, sterile α motif; FL, FLAG-tag; Lin, linker sequence; EPHA2wt, wild-type EPHA2 with aa 24–976; EPHA2ΔEN, EPHA2 lacking aa 29–437; EPHA2ΔFnIIIC, EPHA2 lacking aa 438–527. (B) Binding of DS-8895a to truncated mutants. CT26.WT cells were transfected with FLAG-tagged EPHA2wt, EPHA2ΔEN, and EPHA2ΔFnIIIC. DS-8895a binding and protein expression levels of transfected genes were evaluated by flow cytometry. Human IgG1 and rat IgG2a were used as isotype controls for DS-8895a and anti-FLAG antibody, respectively.

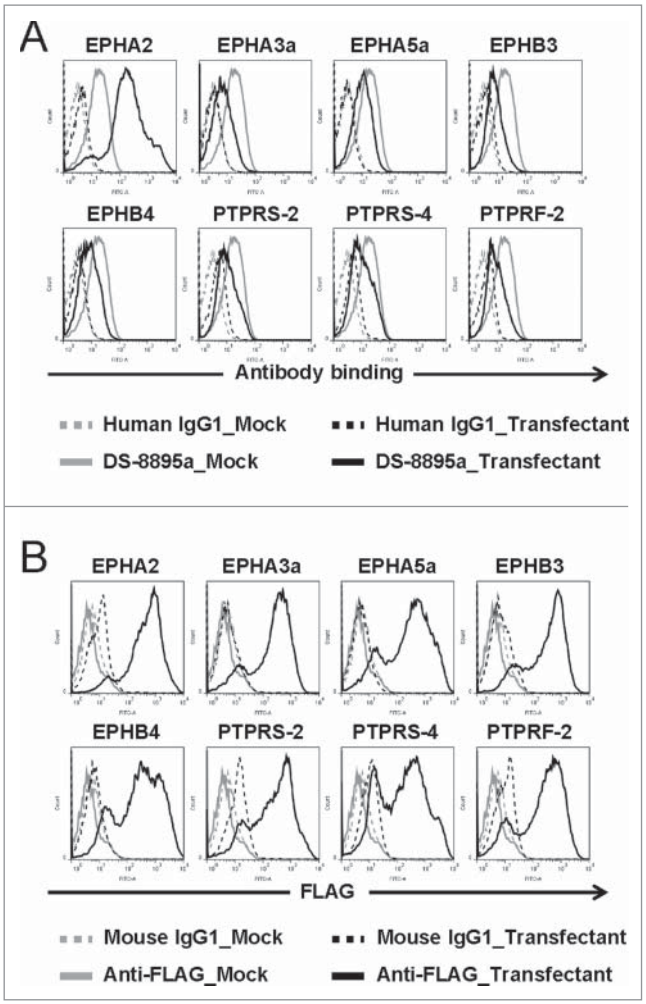

Figure 2. No cross-reactivity of DS-8895a to the human proteins that show high similarity to human EPHA2. 293F cells were transfected with the pFLAG-GW vectors encoding EPHA2 and the human proteins with high amino acid sequence similarity to the region containing the C-terminal FnIII domain of EPHA2 (EPHA3a, EPHA5a, EPHB3, EPHB4, PTPRS-2, PTPRS-4 and PTPRF-2), and the binding of DS-8895a was analyzed by flow cytometer. Transfectant and mock cells represent cells transfected with pFLAG-GW encoding each gene and pFLAG-GW alone, respectively. (A) Mock cells were stained with human IgG1 (gray dashed lines) or DS-8895a (gray solid lines). Cells transfected with each gene were stained with human IgG1 (black dashed lines) or DS-8895a (black solid lines). Human IgG1 was used as a negative control for DS-8895a. (B) Mock cells were stained with mouse IgG1 (gray dashed lines) or anti-FLAG mAb (gray solid lines). Cells transfected with each gene were stained with mouse IgG1 (black dashed lines) or anti-FLAG mAb (black solid lines). Mouse IgG1 was used as a negative control for anti-FLAG mAb. Anti-FLAG mAb staining indicates the cell surface expression of both EPHA2 and the human proteins with high similarity to human EPHA2.

Afucosylated anti-human EPHA2 antibody with enhanced ADCC activity

DS-8895a is humanized IgG1 that is afucosylated to enhance ADCC activity. To compare the ADCC activity of DS-8895a to that of its fucose-containing humanized parent antibody, ADCC assays were conducted using EPHA2-positive MDA-MB-231 cells as target cells and human peripheral blood mononuclear cells (PBMCs) as effector cells. DS-8895a showed markedly increased ADCC activity compared to its parent antibody in the assays using PBMCs from the 2 independent donors (Fig. 4). The half-maximal effective concentration (EC_{50}) values for ADCC activity of DS-8895a were 8.6 and 57.1 ng/mL, where the EC_{50} values of the parent antibody were 105.6 and 821.9 ng/mL in donor A and B, respectively (Fig. 4).

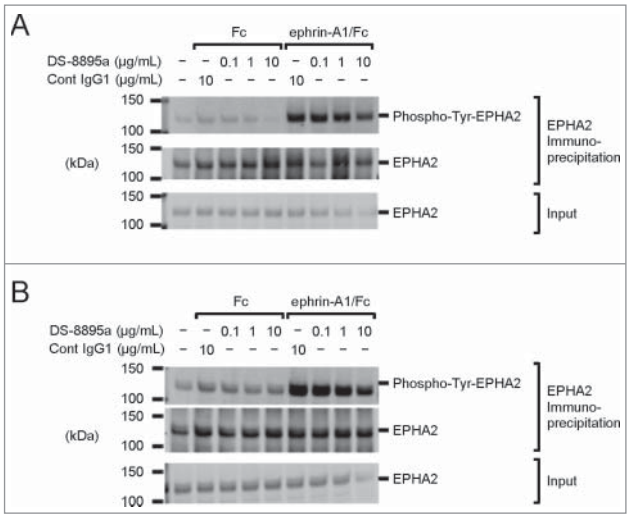

Figure 3. Tyrosine phosphorylation of EPHA2. EPHA2 phosphorylation was examined in (A) MDA-MB-231 and (B) 44As3 cells in the presence and absence of ephrin-A1/Fc and DS-8895a. Fc and cont IgG1 were used as negative controls for ephrin-A1/Fc and DS-8895a, respectively. Cont IgG1, control human IgG1; Phospho-Tyr-EPHA2, tyrosine phosphorylated EPHA2; Input, total cell lysate samples.

Antitumor effects in a breast tumor model

We explored the antitumor activity of DS-8895a in xenograft models. Athymic nude mice were subcutaneously inoculated with EPHA2-positive MDA-MB-231 cells. Immunohistochemical analysis confirmed EPHA2 expression in the xenograft tumors (Fig. 5). In this model, DS-8895a inhibited tumor growth in a dose-dependent manner (Fig. 6, $P < 0.0001$), and the antitumor effect of DS-8895a was statistically significant (0.03 mg/kg: $P = 0.0356$, 0.1 mg/kg: $P = 0.0086$, 0.3, 1, and 3 mg/kg: $P < 0.0001$) when compared with the vehicle group. The result indicates that DS-8895a has potent antitumor activity in the breast cancer model.

Antitumor effects in a gastric tumor model

The antitumor activity of DS-8895a was further evaluated in another xenograft model. Athymic nude mice were subcutaneously inoculated with EPHA2-positive human gastric cancer SNU-16 cells. EPHA2 expression was also confirmed in the xenograft tumors (Fig. 5). In this model, DS-8895a also inhibited tumor growth in a dose-dependent manner (Fig. 7A, $P < 0.0001$). The antitumor effect of DS-8895a at 10 mg/kg was statistically significant when compared with the vehicle group ($P = 0.0006$).

Combination with a chemotherapeutic agent

To evaluate combination with a chemotherapeutic agent in the gastric tumor model, the mice received DS-8895a or cisplatin (CDDP) monotherapy or a combination of both. CDDP alone did not inhibit SNU-16 tumor growth even at the doses of 5 and 10 mg/kg (Fig. 7B, $P = 0.9109$ and $P = 0.2426$, respectively). When a suboptimal dose of DS-8895a (5 mg/kg) was

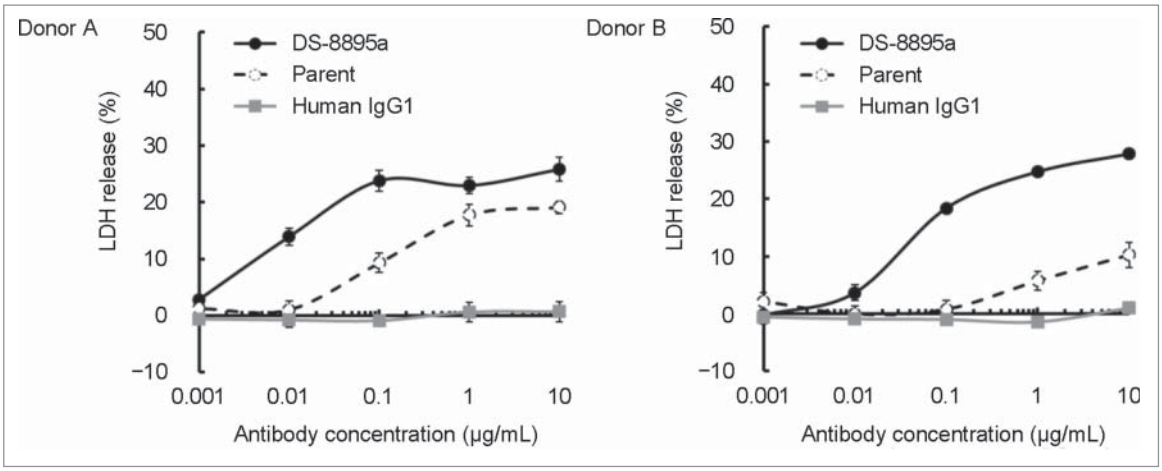

Figure 4. Enhanced ADCC activity of DS-8895a. ADCC assays were conducted using MDA-MB-231 as target cells and human PBMCs as effector cells. The effects of DS-8895a (black filled circles), parent antibody (open circles with a dashed line), and human control IgG1 (gray filled squares) are shown. Data represent the mean ± standard error of the mean. n = 3 for each group, 2 independent donors.

combined with 10 mg/kg of CDDP, combination benefit was observed when compared with monotherapy with individual agent ($P = 0.0284$ for DS-8895a, Dunnett's test and $P = 0.0018$ for CDDP, Student's t-test with Bonferroni correction).

Discussion

EPHA2 is overexpressed in a wide range of cancers and is associated with poor prognosis. EPHA2 upregulation has also been reported in vemurafenib (a BRAF V600E inhibitor)-resistant cancer cells and is involved in the resistance.[33] In addition, truncated membrane-anchoring forms of EPHA2 promote oncogenic signaling.[21,22] These findings indicate the importance of EPHA2 as a target for cancer therapy. We demonstrated that DS-8895a binds to the extracellular juxtamembrane region of EPHA2, as shown in Fig. 1. This result suggests that DS-8895a can target the truncated forms as well as full-length EPHA2 and is effective even in MT1-MMP-positive tumors.

ADCC is mediated by FcγR-expressing NK cells or monocytes/macrophages and thought to be at least in part involved in the therapeutic effects of rituximab, trastuzumab, and cetuximab.[24] Recently, afucosylation of antibody by using a couple of technologies has been shown to increase ADCC.[34] Two afucosylated mAbs with enhanced ADCC have been approved: mogamulizumab, an afucosylated humanized anti-CCR4 mAb (using POTELLIGENT technology) for the treatment of adult T-cell leukemia-lymphoma, peripheral T-cell lymphoma, and cutaneous T-cell lymphoma; obinutuzumab, an afucosylated humanized anti-CD20 mAb (using GlycoMAb technology) for the treatment of chronic lymphocytic leukemia.[25,26]

We produced DS-8895a, an afucosylated anti-EPHA2 mAb to target EPHA2-expressing cancers. Afucosylated DS-8895a exhibited more potent ADCC than its fucose-containing parent antibody (Fig. 4). An afucosylated antibody is reported to induce potent ADCC activity even in the effector cells expressing low-affinity variants of FcγRIIIa (158 valine (V)/phenylalanine (F) or F/F).[35] Moreover, an afucosylated antibody overcomes inhibitory signals induced by the interaction of inhibitory killer cell immunoglobulin-like receptors (KIRs) on effector cells with human leukocyte antigens (HLAs) on target cells, whereas the fucose-containing antibody mediated ADCC is suppressed by them.[36] These evidences support that an afucosylated antibody potentially overcomes the inhibitory effects resulting from the genotypes in FcγRIIIa, KIR, and HLA.

We also demonstrated that DS-8895a significantly inhibited tumor growth in breast and gastric tumor mouse models (Fig. 6 and Fig. 7). Immunohistochemistry for EPHA2 was performed using MDA-MB-231 and SNU-16 xenograft tumors (Fig. 5). Expression levels of EPHA2 were higher in MDA-MB-231 tumors than in SNU-16 tumors. Consistent with the observations, DS-8895a showed stronger antitumor activity in MDA-MB-231 tumors than in SNU-16 tumors (Fig. 6 and Fig. 7). Interestingly, MDA-MB-231 cells used for the studies harbor mutations in KRAS and BRAF.[19] These mutations are associated with aberrant cell signaling and resistance to a variety of therapies.[20] The result also suggests that DS-8895a is effective even in tumors with such mutations since ADCC activity is independent of the tumor signaling pathways.

A BLAST search identified human proteins similar to the region containing the C-terminal FnIII domain of EPHA2. DS-8895a did not bind to those proteins (Fig. 2). This result suggests that DS-8895a specifically binds to EPHA2 and off-target binding is unlikely. DS-8895a also did not bind to mouse EPHA2 (data not shown), suggesting that DS-8895a directly targets inoculated human cancer cells and does not affect mouse cells including EPHA2-expressing vascular endothelial cells in the xenograft models.

Combination of ADCC-mediating antibody with chemotherapeutic agents raises a concern regarding the possible effects of a chemotherapeutic agent on immune cells and the resultant ADCC activity. However, DS-8895a showed increased antitumor activity in the presence of CDDP, and the chemotherapeutic agent did not have a negative impact on the efficacy in the model tested. GA201, an afucosylated anti-EGFR mAb, also showed combination benefit with irinotecan in a mouse xenograft model.[37] These results suggest that ADCC-mediating antibody is potentially effective even in the presence of certain chemotherapeutic agents.

Recently, several studies have suggested that ADCC is associated with not only direct cell killing but also induction of adaptive

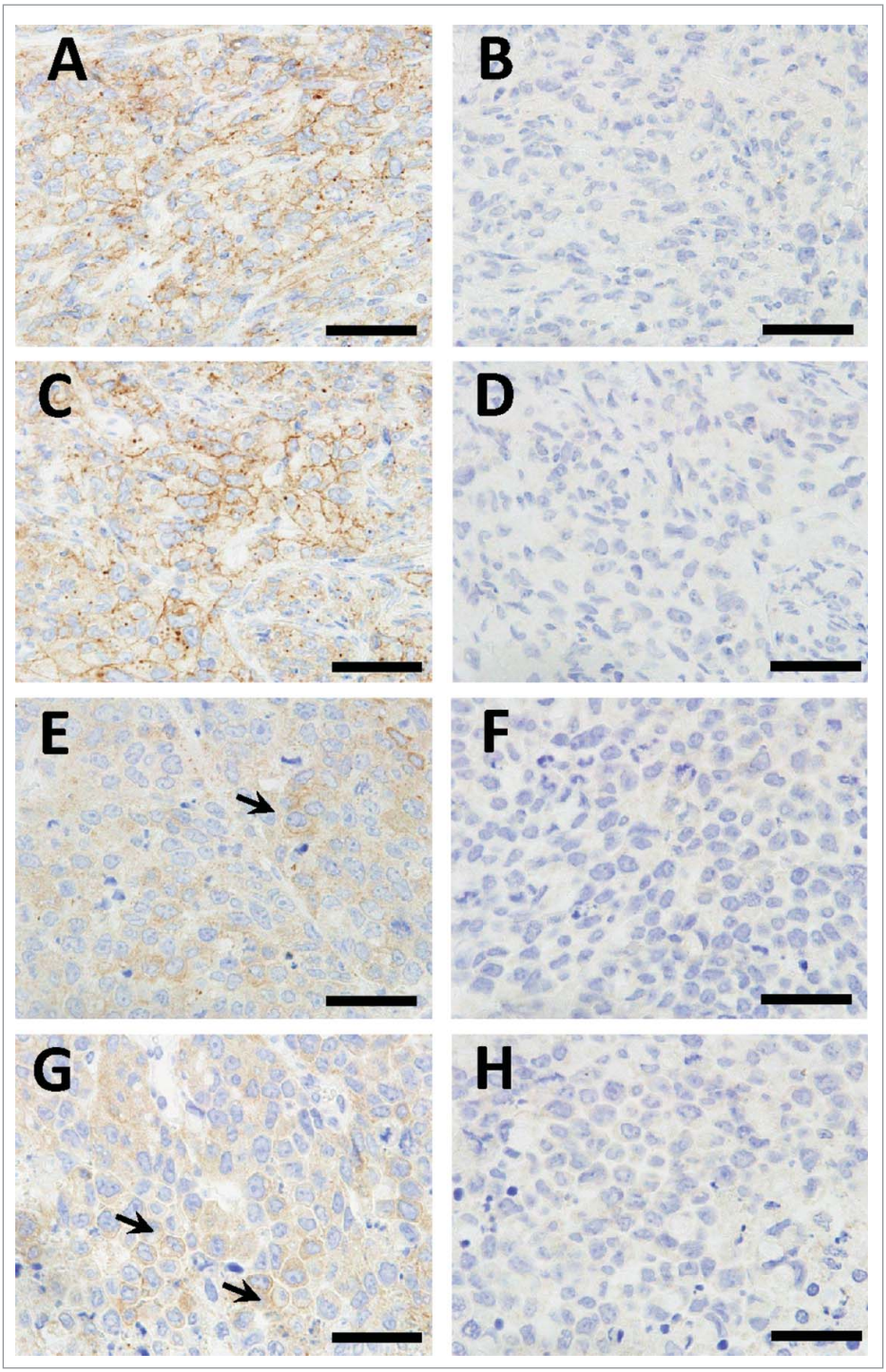

Figure 5. Immunohistochemistry of the xenograft tumors stained with anti-EPHA2 (A, C, E, and G) and Goat IgG (B, D, F, and H). A–D, MDA-MB-231 xenograft tumors; E–H, SNU-16 xenograft tumors. More than half of the tumor cells in the MDA-MB-231 xenograft tumors show weak to moderate membranous EPHA2 staining, while only a few tumor cells show weak membranous EPHA2 staining in the SNU-16 xenograft tumors (arrows). No membranous staining was observed in the xenograft tumors stained with Goat IgG. The bar indicates 50 μm.

immunity to cancer cells. In tumor-bearing mice, macrophage-dependent ADCC by anti-CD20 mAb induced antitumor antigen-specific T cells through the uptake of antigen-antibody complexes by dendritic cells (DCs).[29] Another study showed that increased epidermal growth factor receptor (EGFR)-specific T cells were observed in cetuximab-treated patients with head and neck cancer in comparison to that in cetuximab-naïve patients and that *in vitro*, cetuximab induced DC maturation in an NK cell-dependent manner and promoted cross-presentation by DC to T cells specific not only for EGFR but also for MAGE-3.[38] These data support the concept that ADCC-mediating mAbs can also induce T cell responses specific for tumor antigens.[29,30] However, the activation and activity of tumor-specific T cells are often suppressed by immune checkpoint molecules such as CTLA-4 and PD-1.[39] Thus, ADCC-mediating mAbs may lead to more effective antitumor effects when combined with immune checkpoint inhibitors (e.g. anti-CTLA-4, anti-PD-1, and anti-PD-L1 mAbs). Another approach to enhance the efficacy of ADCC-

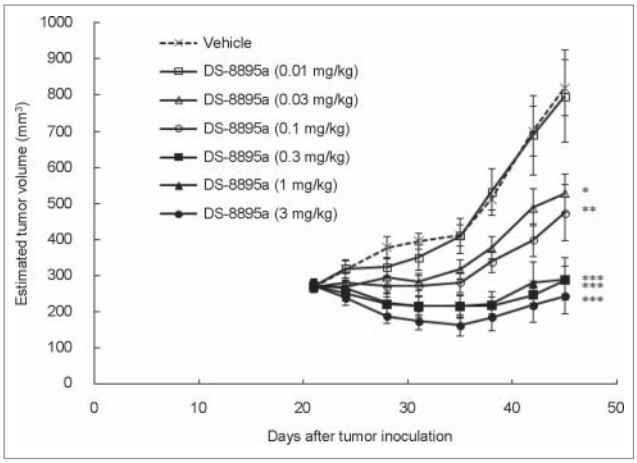

Figure 6. Antitumor activity of DS-8895a in a breast cancer model. Mice (n = 10 per group) were subcutaneously inoculated with MDA-MB-231 cells on day 0. Treatment began on day 21 with different doses of DS-8895a (0.01, 0.03, 0.1, 0.3, 1, and 3 mg/kg, intraperitoneal administration, once a week, 4 injections). Data represent the mean ± standard error. $^{*}P < 0.05$, $^{**}P < 0.01$, $^{***}P < 0.0001$ as compared to the vehicle group (day 45, Dunnett's test).

mediating mAbs is combination with an agonist for co-stimulatory molecules. In particular, anti-CD137 agonistic mAb enhanced rituximab-, trastuzumab-, and cetuximab-mediated ADCC and showed combination benefits with these ADCC-mediating mAbs in tumor-bearing mice.[40-42] These combination approaches are expected to be more suitable for ADCC-enhancing mAbs such as DS-8895a than for fucose-containing ADCC-mediating mAbs.

Taken together, the novel afucosylated anti-EPHA2 mAb, DS-8895a, showed increased *in vitro* ADCC activity and antitumor effects in mouse xenograft models. DS-8895a is expected to be effective for the treatment of patients with EPHA2-positive malignant tumors and is currently under clinical development.

Materials and methods

Antibodies

Mice were immunized with recombinant human EPHA2, and the obtained mouse anti-EPHA2 antibody was humanized as human IgG1. The obtained humanized antibody was afucosylated using POTELLIGENT technology from BioWa, Inc.

Cells

The human breast cancer cell line, MDA-MB-231, the human gastric cancer cell line, SNU-16, and the mouse colon carcinoma cell line CT26.WT were purchased from the American Type Culture Collection. The human gastric cancer cell line 44As3 was obtained from Yasuda Women's University.[43] MDA-MB-231 cells were cultured in Leibovitz's L-15 (Thermo Fisher Scientific) or RPMI1640 (Thermo Fisher Scientific) both supplemented with 10% heat-inactivated fetal bovine serum (FBS, Thermo Fisher Scientific) at 37°C in a humidified atmosphere without CO_2 (Leibovitz's L-15) or in a humidified atmosphere of 5% CO_2 (RPMI1640). SNU-16, CT26.WT, and 44As3 cells were cultured in RPMI1640 supplemented with 10% heat-inactivated FBS at 37°C in a humidified atmosphere of 5% CO_2. The 293F cells (Thermo Fisher Scientific, R790-07) were cultured in FreeStyle 293 Expression Medium (Thermo Fisher Scientific, 12338-018) at 37°C in a humidified atmosphere of 8% CO_2 with shaking at 135 rpm.

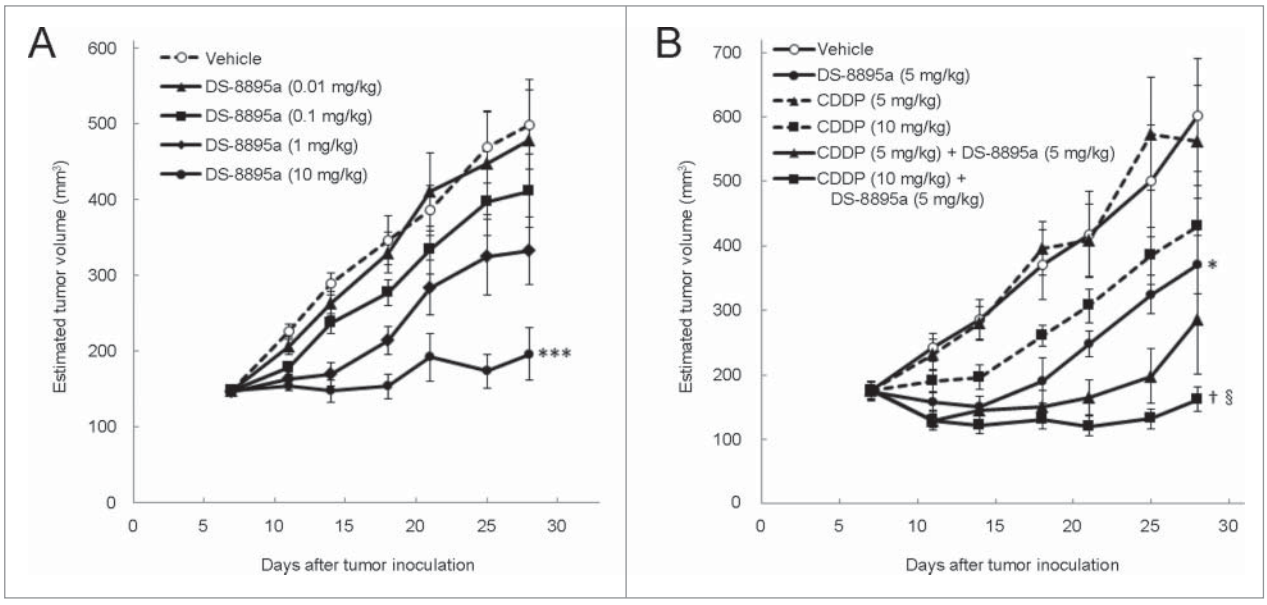

Figure 7. Antitumor activity of DS-8895a in a gastric cancer model. Mice were subcutaneously inoculated with SNU-16 cells on day 0. (A) Treatment began on day 7 with different doses of DS-8895a (0.01, 0.1, 1, and 10 mg/kg, intraperitoneal administration, once a week, 3 injections). Data represent the mean ± standard error. $^{***}P < 0.001$ as compared to the vehicle group (day 28, Dunnett's test). n = 10 per group. (B) Treatment began on day 7 with DS-8895a (5 mg/kg, intravenous administration, once a week, 3 injections), CDDP (5 and 10 mg/kg, intravenous administration, single injection), and DS-8895a (5 mg/kg, intravenous administration, once a week, 3 injections) in combination with CDDP (5 or 10 mg/kg, intravenous administration, single injection). Data represent the mean ± standard error. $^{*}P < 0.05$ as compared to the vehicle group (day 28, Student's t-test). †$P < 0.05$ as compared to the DS-8895a (5 mg/kg) monotherapy group (day 28, Dunnett's test). §$P < 0.01$ as compared to the CDDP (10 mg/kg) monotherapy group (day 28, Student's t-test with Bonferroni correction). n = 9 per group.

Constructs

To construct a destination vector, Reading Frame Cassette B (RfB) of Gateway Vector Conversion System (Thermo Fisher Scientific) was ligated into blunt-ended HindIII and BglII sites of pFLAG-myc-CMV-19 (Sigma-Aldrich). The resultant vector was designated pFLAG-GW. To generate plasmids expressing wild-type and mutant EPHA2, AttB sites were incorporated into EPHA2wt (aa 24–976 and stop codon]), EPHA2ΔEN (aa 24–28, aa 438–976, and stop codon), and EPHA2ΔFnIIIC (aa 24–437, aa 528–976, and stop codon) by PCR reactions using the following primers: EPHA2wt forward, 5′-GGGGACAAGTTTGTACAAAAAAGCAGGCTCAGCGCAGGGCAAGGAAG-3′; EPHA2wt reverse, 5′-GGGGACCACTTTGTACAAGAAAGCTGGGTCTCAGATGGGGATCCCCAC-3′; EPHA2ΔEN3 forward, 5′-GGGGACAAGTTTGTACAAAAAAGCAGGCTCAGCGCAGGGCAAGGAAGAGCC-3′; EPHA2ΔEN3 reverse, 5′-GGGGACCACTTTGTACAAGAAAGCTGGGTCTCAGATGGGGATCCCCACAGTGTTC-3′; EPHA2ΔFnIIIC forward, 5′-GGGGACAAGTTTGTACAAAAAAGCAGGCTCAGCGCAGGGCAAGGAAGTGG-3′; EPHA2ΔFnIIIC reverse, 5′-GGGGACCACTTTGTACAAGAAAGCTGGGTCTCAGATGGGGATCCCCACAGTGTTC-3′. The underlines represent the coding regions of EPHA2, and the double underlines represent stop codons. The PCR fragments were cloned into pDONR221 (Thermo Fisher Scientific) by BP reactions and then transferred to pFLAG-GW by LR reactions. The resultant vectors were designated pFLAG-EPHA2wt, pFLAG-EPHA2ΔEN, and pFLAG-EPHA2ΔFnIIIC. A BLAST search (BLASTP 2.2.22+)[44] was performed to identify human proteins with high amino acid sequence similarity to the region containing the C-terminal FnIII domain of human EPHA2. To generate plasmids expressing the identified genes: EPHA3 isoform a (EPHA3a), EPHA5 isoform a (EPHA5a), EPHB3, EPHB4, PTPRS isoform 2 (PTPRS-2), PTPRS isoform 4 (PTPRS-4), and PTPRF isoform 2 (PTPRF-2), AttB sites were incorporated into the genes by PCR reactions using the following primers: EPHA3a forward, 5′-GGGGACAAGTTTGTACAAAAAAGCAGGCTCAGAACTGATTCCGCAGCCT-3′; EPHA3a reverse, 5′-GGGGACCACTTTGTACAAGAAAGCTGGGTCTTACACGGGAACTGGGCC-3′; EPHA5a forward, 5′-GGGGACAAGTTTGTACAAAAAAGCAGGCTTCAGCCCCAGCAACGAAGTGAATTTATTGG-3′; EPHA5a reverse, 5′-GGGGACCACTTTGTACAAGAAAGCTGGGTCTTACAATGGCACCATTCCGTTTACCAG-3′; EPHB3 forward, 5′-GGGGACAAGTTTGTACAAAAAAGCAGGCTCACTGGAAGAGACCCTCATG-3′; EPHB3 reverse, 5′-GGGGACCACTTTGTACAAGAAAGCTGGGTCTCAGACCTGCACAGGCAG-3′; EPHB4 forward, 5′-GGGGACAAGTTTGTACAAAAAAGCAGGCTCATTGGAAGAGACCCTGCTG-3′; EPHB4 reverse, 5′-GGGGACCACTTTGTACAAGAAAGCTGGGTCTCAGTACTGCGGGGCCG-3′; PTPRS-2/PTPRS-4 forward, 5′-GGGGACAAGTTTGTACAAAAAAGCAGGCTTCGAAGAGCCCCCCAGGTTTATC-3′; PTPRS-2/PTPRS-4 reverse, 5′-GGGGACCACTTTGTACAAGAAAGCTGGGTCTTAGGTTGCATAGTGGTCAAAG-3′; PTPRF-2 forward, 5′-GGGGACAAGTTTGTACAAAAAAGCAGGCTTCGACAGCAAACCTGTCTTCATTAAAG-3′; PTPRF-2 reverse, 5′-GGGGACCACTTTGTACAAGAAAGCTGGGTCTTACGTTGCATAGTGGTCAAAGCTG-3′. The underlines represent the coding regions of the genes, and the double underlines represent stop codons. The PCR fragments were cloned into pDONR221 by BP reactions and then transferred to pFLAG-GW by LR reactions. The resultant vectors were designated pFLAG-EPHA3a, pFLAG-EPHA5a, pFLAG-EPHB3, pFLAG-EPHB4, pFLAG-PTPRS-2, pFLAG-PTPRS-4, and pFLAG-PTPRF-2. Analysis of conserved domains was performed using the human EPHA2 sequence (GeneBank Accession Number NM_004431.3). The signal peptide cleavage site and the transmembrane domain of EPHA2 were predicted by SignalP v. 3.0 and TMHMM Server v. 2.0, respectively.[45,46] The other conserved domains of EPHA2 were predicted by NCBI's CD-search.[47]

Transfection, cell staining, and flow cytometry

CT26.WT cells were transfected with pFLAG-EPHA2wt, pFLAG-EPHA2ΔEN, and pFLAG-EPHA2ΔFnIIIC by using Lipofectamine 2000 (Thermo Fisher Scientific). The transfected and non-transfected CT26.WT cells were stained with 5 μg/mL DS-8895a, 5 μg/mL human IgG1 (an isotype control for DS-8895a, Eureka Therapeutics, ET901), 1 μg/mL PE-labeled anti-FLAG mAb (Biolegend, 637309), or 1 μg/mL PE-labeled rat IgG2a κ (an isotype control for anti-FLAG mAb, Biolegend, 400507). The cells stained with DS-8895a or human IgG1 were further stained with APC-labeled $F(ab')_2$ of goat anti-human IgG, Fcγ fragment specific (Jackson ImmunoResearch, 109-136-170). To discriminate dead cells, the cells were stained using LIVE/DEAD Fixable Far Red Dead Cell Stain Kit (Thermo Fisher Scientific). and then fixed with BD FACS Lysing Solution (Becton, Dickinson and Company). 293F cells were transfected with pFLAG-EPHA2wt, pFLAG-EPHA3a, pFLAG-EPHA5a, pFLAG-EPHB3, pFLAG-EPHB4, pFLAG-PTPRS-2, pFLAG-PTPRS-4, pFLAG-PTPRF-2, and pFLAG-GW using 293fectin reagent (Thermo Fisher Scientific, 12347019). pFLAG-GW was used as a negative (mock) control. Two days after the transfection, cells were stained with 10 μg/mL of DS-8895a, human IgG1 (an isotype control for DS-8895a, Enzo Life Sciences, ALX-804-133-C100), monoclonal ANTI-FLAG M2 antibody (anti-FLAG mAb, Sigma-Aldrich, F1804), or mouse IgG1 (an isotype control for anti-FLAG mAb, Becton, Dickinson and Company, 554721). Cells were then stained with fluorescein isothiocyanate (FITC)-conjugated anti-human IgG (Jackson ImmunoResearch Laboratories, 109-096-088) for DS-8895a and human IgG1 or FITC-conjugated anti-mouse IgG (MP Biomedicals, 55493) for anti-FLAG mAb and mouse IgG1 and then stained with 7-AAD (Thermo Fisher Scientific, A1310). The stained cells were analyzed on BD FACS Canto II (Becton, Dickinson and Company). Data analysis was performed using FlowJo version 7.6.5 (Tree Star, Inc.).

Western blotting and immunoprecipitation

MDA-MB-231 and 44As3 cells were seeded into 12-well plates and cultured overnight in Leibovitz's L-15 containing 10% heat inactivated FBS at 37°C in a humidified atmosphere without CO_2 and in RPMI1640 containing 10% heat inactivated FBS at 37°C in a humidified atmosphere of 5% CO_2, respectively. The next day, culture media were removed, and cells were starved

in Leibovitz's L-15 (MDA-MB-231) and RPMI1640 (44As3) both without FBS overnight. After removing the starvation media, cells were treated with DS-8895a and control human IgG1 (Enzo Life Sciences) at the concentrations shown in Fig. 3 for 1 h and then stimulated with 1 μg/mL of human Ephrin-A1 Fc (ephrin-A1/Fc, R&D Systems, 6417-A1) or human IgG1 Fc (Fc, R&D Systems, 110-HG-100) for 15 min at 37°C. Cells were lysed with cell lysis buffer (RIPA buffer [Sigma-Aldrich, R0278-500ML] containing PhosSTOP [Roche Diagnostics, 04 906 837 001] and Complete mini [Roche Diagnostics, 04 693 124 001]) and then spun down to obtain clear total cell lysates. Protein A magnetic beads (25 μL/sample, New England BioLabs, S1425S) were incubated with anti-EPHA2-antibody (8 μg/sample, C-20, Santa Cruz biotechnology, sc-924) at 4°C for about 3 h and then blocked by a further 30 min incubation at 4°C in the presence of 10% FBS. After washing the beads with RIPA buffer 3 times, the beads were incubated with the clear cell lysate at 4°C for 3 h with rotation and then washed with RIPA buffer 3 times. The immunoprecipitated proteins and total cell lysate (input) were separated by SDS-PAGE and transferred to the Immobilon-FL PVDF membrane (EMD MILLIPORE, IPFL00010). The membrane was probed with anti-phosphotyrosine (4G10, EMD MILLIPORE, 05-321) followed by a secondary antibody, IRDye 800CW Goat Anti-mouse IgG (LI-COR Biosciences, 926-32210). The same membrane was then probed with anti-EPHA2 antibody (C-20) followed by IRDye 680 Goat Anti-Rabbit IgG (LI-COR Biosciences, 926-32221). The fluorescence signals were detected by ODYSSEY (LI-COR Biosciences).

ADCC assay

PBMCs were isolated from heparinized blood of healthy donors via density gradient centrifugation using ficoll-paque plus (GE Healthcare). Written informed consent was obtained from all healthy volunteers in accordance with the Daiichi Sankyo Ethics Committee. MDA-MB-231 cells (1×10^4 cells/well) as target cells were cultured overnight in 96-well plates in ADCC media (phenol red free RPMI1640 [Thermo Fisher Scientific] containing 10% FBS and penicillin/streptomycin [Thermo Fisher Scientific]). The next day, the target cells were incubated with DS-8895a or human IgG1 (Enzo Life Sciences, ALX-804-133-C100) for 1 hour at room temperature and then further incubated with 2.5×10^4 cells/well of PBMCs (effector:target = 25:1) at 37°C in a humidified atmosphere of 5% CO_2 for 16 hours. The final concentrations of each reagent are shown in Fig. 4. Lysis of target cells was determined by evaluating lactate dehydrogenase (LDH) release (excitation/emission = 540/590 nm) using CytoTox-ONE reagent Homogeneous Membrane Integrity Assay (Promega). The percent specific LDH release was calculated using the following equation:

$$\text{Specific LDH release (\%)} = (x - a)/(b - a) \times 100$$

x is the fluorescence intensity of a test well, a is the mean fluorescence intensity under spontaneous release, and b is the mean fluorescence intensity under maximum release from Triton X-100-lysed target cells. The assay was conducted in triplicate.

EC_{50} values of DS-8895a and its parent antibody were estimated according to the Sigmoid Emax model that is defined by the following equation.

[Sigmoid Emax model]

$$\text{Specific LDH release (\%)} = \frac{(E_{max} - E_0) \times [Conc]^{\gamma}}{[EC_{50}]^{\gamma} + [Conc]^{\gamma}} + E_0$$

E_0: response when dose is 0 (vehicle control, $E_0 = 0$)

E_{max}: mean maximal response (percent of specific LDH release at 10 μg/mL of antibodies).

Conc: concentration of DS-8895a or parent antibody (μg/mL)

EC_{50}: the concentration of DS-8895a or its parent antibody at which specific LDH release (%) was equal to $(E_0 + E_{max})/2$ (μg/mL)

γ: sigmoidicity factor

EC_{50} values (μg/mL) were rounded to 4 decimal places and expressed in ng/mL. Statistical analyses were performed using SAS System Release 8.2 (SAS Institute Inc.).

Mouse xenograft models

Female nude mice (CAnN.Cg-*Foxn1*^{nu}/CrlCrlj [nu/nu], 5-week-old) were purchased from Charles River Laboratories Japan, Inc. and housed under specific pathogen-free conditions. All animal experiments in this study were performed in accordance with the in-house guidelines of the Institutional Animal Care and Use Committee of Daiichi Sankyo Co., Ltd. Mice were subcutaneously inoculated with 5×10^6 MDA-MB-231 cells or 5×10^6 SNU-16 cells suspended in 0.1 mL 100% or 50% BD Matrigel Basement Membrane Matrix (Becton, Dickinson and Company), respectively (day 0). Tumor length and width were measured using a digital caliper, and estimated tumor volume was calculated by the following equation.

$$\text{Estimated tumor volume}\left(\text{mm}^3\right) = 1/2 \times [\text{tumor length(mm)}] \times [\text{tumor width(mm)}]^2$$

The mice were randomized into the indicated number of groups on day 21 (for MDA-MB-231 tumors) or day 7 (for SUN-16 tumors) according to the estimated tumor volume. CDDP was purchased from Nippon Kayaku Co., Ltd. Mice received treatment as described in Figs. 6 and 7 from day 21 and day 7, respectively.

Immunohistochemistry (IHC)

Female nude mice bearing MDA-MB-231 and SNU-16 tumors were euthanized by cervical dislocation under anesthesia, and subcutaneous tumors were dissected. After dissection, tumor tissues were fixed with 10% neutral buffed formalin (Mildform®10N, Wako Pure Chemicals, 133-10311) for 2 days, and processed for standard formalin-fixed paraffin-embedded sections. IHC was performed using Autostainer Link 48 (DAKO) and PT Link (DAKO) at room temperature, unless otherwise stated. All of the primary antibodies (Goat anti-EPHA2 Ab [R&D Systems, AF3035] and Normal goat IgG [R&D Systems, AB-108-C]) were diluted to a final concentration of 2.5 μg/mL with the DAKO REAL Antibody Diluent

(DAKO, S2022). Approximately 4 μm thick sections were deparaffinized and pretreated with Envision FLEX TRS High (DAKO, K8004) for 40 min at 97°C followed by endogenous peroxidase blocking (DAKO, S2023) and protein blocking (DAKO, X0909). Then, the sections were sequentially incubated with the primary antibodies for 1 h, Histofine Simple Stain MAX-PO (Goat) (Nichirei Bioscience, 414161) as a secondary antibody for 30 min, and DAB+ Liquid (DAKO, K3468) for 10 min. Washes were performed after every step. Finally, the sections were counterstained with EnVision FLEX Hematoxylin (DAKO, K8008) for 5 min, and mounted. Two individual tumors from each xenograft model were used for IHC.

Statistical analysis

The dose-response relationship was evaluated by a Spearman's rank correlation coefficient hypothesis test (null hypothesis: correlation coefficient = 0). In the combination study with CDDP, statistical analysis was performed with Student's t-test (the vehicle group versus the DS-8895a monotherapy group), Dunnett's test (the vehicle group vs. the CDDP monotherapy groups, and the DS-8895a monotherapy group versus DS-8895a and CDDP-treated groups), and Student's t-test with Bonferroni correction (each CDDP monotherapy group vs. each DS-8895a and CDDP-treated group). A *P* value of less than 0.05 (2-sided) was considered statistically significant. All the statistical analyses were performed using SAS System Release 8.2.

Disclosure of potential conflict of interests

J.H., M.S., M.Y., J.I., S.I., T.S., M.K., T.W., and T.A. are employees of Daiichi Sankyo Co., Ltd.

Acknowledgments

We would like to thank Toshiaki Ohtsuka and Tohru Takahashi for their critical advice and helpful discussions, Chigusa Yoshimura for establishment of anti-EPHA2 mAbs, Atsushi Urano, Junko Yamaguchi, Naoki Wada, Yuri Tominaga, Hironobu Komori, and Toshiyuki Kosaka for screening and characterization of anti-EPHA2 mAbs, Tatsuji Matsuoka, Makiko Nakayama, Takeshi Takizawa and Hiroyuki Hanzawa for cloning of anti-EPHA2 mAb genes and their humanization, Masato Yamanobe, Toshinori Ohmine, and Kenji Miyadai for the production of DS-8895a, and the rest of our colleagues at Daiichi Sankyo Co., Ltd. and Daiichi Sankyo RD Novare Co., Ltd.

References

1. Orioli D, Klein R. The Eph receptor family: axonal guidance by contact repulsion. Trends Genet 1997; 13:354-9; PMID:9287490; http://dx.doi.org/10.1016/S0168-9525(97)01220-1
2. Yuan WJ, Ge J, Chen ZK, Wu SB, Shen H, Yang P, Hu B, Zhang GW, Chen ZH. Over-expression of EphA2 and EphrinA-1 in human gastric adenocarcinoma and its prognostic value for postoperative patients. Dig Dis Sci 2009; 54:2410-7; PMID:19101799; http://dx.doi.org/10.1007/s10620-008-0649-4
3. Saito T, Masuda N, Miyazaki T, Kanoh K, Suzuki H, Shimura T, Asao T, Kuwano H. Expression of EphA2 and E-cadherin in colorectal cancer: correlation with cancer metastasis. Oncol Rep 2004; 11:605-11; PMID:14767510; http://dx.doi.org/10.3892/or.11.3.605
4. Dunne PD, Dasgupta S, Blayney JK, McArt DG, Redmond KL, Weir JA, Bradley CA, Sasazuki T, Shirasawa S, Wang T, et al. EphA2 expression is a key driver of migration and invasion and a poor prognostic marker in colorectal cancer. Clin Cancer Res 2016; 22:230-42; PMID:26283684; http://dx.doi.org/10.1158/1078-0432.CCR-15-0603
5. Miyazaki T, Kato H, Fukuchi M, Nakajima M, Kuwano H. EphA2 overexpression correlates with poor prognosis in esophageal squamous cell carcinoma. Int J Cancer 2003; 103:657-63; PMID:12494475; http://dx.doi.org/10.1002/ijc.10860
6. Brannan JM, Dong W, Prudkin L, Behrens C, Lotan R, Bekele BN, Wistuba I, Johnson FM. Expression of the receptor tyrosine kinase EphA2 is increased in smokers and predicts poor survival in non-small cell lung cancer. Clin Cancer Res 2009; 15:4423-30; PMID:19531623; http://dx.doi.org/10.1158/1078-0432.CCR-09-0473
7. Zelinski DP, Zantek ND, Stewart JC, Irizarry AR, Kinch MS. EphA2 overexpression causes tumorigenesis of mammary epithelial cells. Cancer Res 2001; 61:2301-6; PMID:11280802
8. Cui XD, Lee MJ, Yu GR, Kim IH, Yu HC, Song EY, Kim DG. EFNA1 ligand and its receptor EphA2: potential biomarkers for hepatocellular carcinoma. Int J Cancer 2010; 126:940-9; PMID:19642143; http://dx.doi.org/10.1002/ijc.24798
9. Zeng G, Hu Z, Kinch MS, Pan CX, Flockhart DA, Kao C, Gardner TA, Zhang S, Li L, Baldridge LA, et al. High-level expression of EphA2 receptor tyrosine kinase in prostatic intraepithelial neoplasia. Am J Pathol 2003; 163:2271-6; PMID:14633601; http://dx.doi.org/10.1016/S0002-9440(10)63584-5
10. Thaker PH, Deavers M, Celestino J, Thornton A, Fletcher MS, Landen CN, Kinch MS, Kiener PA, Sood AK. EphA2 expression is associated with aggressive features in ovarian carcinoma. Clin Cancer Res 2004; 10:5145-50; PMID:15297418; http://dx.doi.org/10.1158/1078-0432.CCR-03-0589
11. Mudali SV, Fu B, Lakkur SS, Luo M, Embuscado EE, Iacobuzio-Donahue CA. Patterns of EphA2 protein expression in primary and metastatic pancreatic carcinoma and correlation with genetic status. Clin Exp Metastasis 2006; 23:357-65; PMID:17146615; http://dx.doi.org/10.1007/s10585-006-9045-7
12. Abraham S, Knapp DW, Cheng L, Snyder PW, Mittal SK, Bangari DS, Kinch M, Wu L, Dhariwal J, Mohammed SI. Expression of EphA2 and Ephrin A-1 in carcinoma of the urinary bladder. Clin Cancer Res 2006; 12:353-60; PMID:16428472; http://dx.doi.org/10.1158/1078-0432.CCR-05-1505
13. Holm R, de Putte GV, Suo Z, Lie AK, Kristensen GB. Expressions of EphA2 and EphrinA-1 in early squamous cell cervical carcinomas and their relation to prognosis. Int J Med Sci 2008; 5:121-6; PMID:18566674; http://dx.doi.org/10.7150/ijms.5.121
14. Merritt WM, Kamat AA, Hwang JY, Bottsford-Miller J, Lu C, Lin YG, Coffey D, Spannuth WA, Nugent E, Han LY, et al. Clinical and biological impact of EphA2 overexpression and angiogenesis in endometrial cancer. Cancer Biol Ther 2010; 10:1306-14; PMID:20948320; http://dx.doi.org/10.4161/cbt.10.12.13582
15. Herrem CJ, Tatsumi T, Olson KS, Shirai K, Finke JH, Bukowski RM, Zhou M, Richmond AL, Derweesh I, Kinch MS, et al. Expression of EphA2 is prognostic of disease-free interval and overall survival in surgically treated patients with renal cell carcinoma. Clin Cancer Res 2005; 11:226-31; PMID:15671550
16. Wang LF, Fokas E, Bieker M, Rose F, Rexin P, Zhu Y, Pagenstecher A, Engenhart-Cabillic R, An HX. Increased expression of EphA2 correlates with adverse outcome in primary and recurrent glioblastoma multiforme patients. Oncol Rep 2008; 19:151-6; PMID:18097589; http://dx.doi.org/10.3892/or.19.1.151
17. Liu Y, Zhang X, Qiu Y, Huang D, Zhang S, Xie L, Qi L, Yu C, Zhou X, Hu G, et al. Clinical significance of EphA2 expression in squamous-cell carcinoma of the head and neck. J Cancer Res Clin Oncol 2011; 137:761-9; PMID:20614133; http://dx.doi.org/10.1007/s00432-010-0936-2
18. Straume O, Akslen LA. Importance of vascular phenotype by basic fibroblast growth factor, and influence of the angiogenic factors basic fibroblast growth factor/fibroblast growth factor receptor-1 and ephrin-A1/EphA2 on melanoma progression. Am J Pathol 2002; 160:1009-19; PMID:11891198; http://dx.doi.org/10.1016/S0002-9440(10)64922-X

19. Macrae M, Neve RM, Rodriguez-Viciana P, Haqq C, Yeh J, Chen C, Gray JW, McCormick F. A conditional feedback loop regulates Ras activity through EphA2. Cancer Cell 2005; 8:111-8; PMID:16098464; http://dx.doi.org/10.1016/j.ccr.2005.07.005
20. Dhillon AS, Hagan S, Rath O, Kolch W. MAP kinase signalling pathways in cancer. Oncogene 2007; 26:3279-90; PMID:17496922; http://dx.doi.org/10.1038/sj.onc.1210421
21. Koshikawa N, Hoshino D, Taniguchi H, Minegishi T, Tomari T, Nam SO, Aoki M, Sueta T, Nakagawa T, Miyamoto S, et al. Proteolysis of EphA2 converts it from a tumor suppressor to an oncoprotein. Cancer Res 2015; 75:3327-39; PMID:26130649; http://dx.doi.org/10.1158/0008-5472.CAN-14-2798
22. Sugiyama N, Gucciardo E, Tatti O, Varjosalo M, Hyytiäinen M, Gstaiger M, Lehti K. EphA2 cleavage by MT1-MMP triggers single cancer cell invasion via homotypic cell repulsion. J Cell Biol 2013; 201:467-84; PMID:23629968; http://dx.doi.org/10.1083/jcb.201205176
23. Scott AM, Wolchok JD, Old LJ. Antibody therapy of cancer. Nat Rev Cancer 2012; 12:278-87; PMID:22437872; http://dx.doi.org/10.1038/nrc3236
24. Seidel UJE, Schlegel P, Lang P. Natural killer cell mediated antibody-dependent cellular cytotoxicity in tumor immunotherapy with therapeutic antibodies. Front Immunol 2013; 4:76; PMID:23543707; http://dx.doi.org/10.3389/fimmu.2013.00076
25. Remer M, Al-Shamkhani A, Glennie M, Johnson P. Mogamulizumab and the treatment of CCR4-positive T-cell lymphomas. Immunotherapy 2014; 6:1187-206; PMID:25496334; http://dx.doi.org/10.2217/imt.14.94
26. Goede V, Klein C, Stilgenbauer S. Obinutuzumab (GA101) for the treatment of chronic lymphocytic leukemia and other B-cell non-hodgkin's lymphomas: a glycoengineered type II CD20 antibody. Oncol Res Treat 2015; 38:185-92; PMID:25877943; http://dx.doi.org/10.1159/000381524
27. Stewart R, Hammond SA, Oberst M, Wilkinson RW. The role of Fc gamma receptors in the activity of immunomodulatory antibodies for cancer. J Immunother Cancer 2014; 2:29; http://dx.doi.org/10.1186/s40425-014-0029-x
28. Trapani JA, Smyth MJ. Functional significance of the perforin/granzyme cell death pathway. Nat Rev Immunol 2002; 2:735-47; PMID:12360212; http://dx.doi.org/10.1038/nri911
29. DiLillo DJ, Ravetch JV. Differential Fc-receptor engagement drives an anti-tumor vaccinal effect. Cell 2015; 161:1035-45; PMID:25976835; http://dx.doi.org/10.1016/j.cell.2015.04.016
30. DiLillo DJ, Ravetch JV. Fc-receptor interactions regulate both cytotoxic and immunomodulatory therapeutic antibody effector functions. Cancer Immunol Res 2015; 3:704-13; PMID:26138698; http://dx.doi.org/10.1158/2326-6066.CIR-15-0120
31. Shields RL, Lai J, Keck R, O'Connell LY, Hong K, Meng YG, Weikert SHA, Presta LG. Lack of fucose on human IgG1 N-linked oligosaccharide improves binding to human Fcgamma RIII and antibody-dependent cellular toxicity. J Biol Chem 2002; 277:26733-40; PMID:11986321; http://dx.doi.org/10.1074/jbc.M202069200
32. Shinkawa T, Nakamura K, Yamane N, Shoji-Hosaka E, Kanda Y, Sakurada M, Uchida K, Anazawa H, Satoh M, Yamasaki M, et al. The absence of fucose but not the presence of galactose or bisecting N-acetylglucosamine of human IgG1 complex-type oligosaccharides shows the critical role of enhancing antibody-dependent cellular cytotoxicity. J Biol Chem 2003; 278:3466-73; PMID:12427744; http://dx.doi.org/10.1074/jbc.M210665200
33. Miao B, Ji Z, Tan L, Taylor M, Zhang J, Choi HG, Frederick DT, Kumar R, Wargo JA, Flaherty KT, et al. EPHA2 is a mediator of vemurafenib resistance and a novel therapeutic target in melanoma. Cancer Discov 2015; 5:274-87; PMID:25542448; http://dx.doi.org/10.1158/2159-8290.CD-14-0295
34. Beck A, Reichert JM. Marketing approval of mogamulizumab: a triumph for glyco-engineering. MAbs 2012; 4:419-25; PMID:22699226; http://dx.doi.org/10.4161/mabs.20996
35. Niwa R, Hatanaka S, Shoji-Hosaka E, Sakurada M, Kobayashi Y, Uehara A, Yokoi H, Nakamura K, Shitara K. Enhancement of the antibody-dependent cellular cytotoxicity of low-fucose IgG1 is independent of FcgammaRIIIa functional polymorphism. Clin Cancer Res 2004; 10:6248-55; PMID:15448014; http://dx.doi.org/10.1158/1078-0432.CCR-04-0850
36. Terszowski G, Klein C, Stern M. KIR/HLA interactions negatively affect rituximab- but not GA101 (obinutuzumab)-induced antibody-dependent cellular cytotoxicity. J Immunol 2014; 192:5618-24; PMID:24795454; http://dx.doi.org/10.4049/jimmunol.1400288
37. Gerdes CA, Nicolini VG, Herter S, van Puijenbroek E, Lang S, Roemmele M, Moessner E, Freytag O, Friess T, Ries CH, et al. GA201 (RG7160): a novel, humanized, glycoengineered anti-EGFR antibody with enhanced ADCC and superior in vivo efficacy compared with cetuximab. Clin Cancer Res 2013; 19:1126-38; PMID:23209031; http://dx.doi.org/10.1158/1078-0432.CCR-12-0989
38. Srivastava RM, Lee SC, Andrade Filho PA, Lord CA, Jie HB, Davidson HC, López-Albaitero A, Gibson SP, Gooding WE, Ferrone S, et al. Cetuximab-activated natural killer and dendritic cells collaborate to trigger tumor antigen-specific T-cell immunity in head and neck cancer patients. Clin Cancer Res 2013; 19:1858-72; PMID:23444227; http://dx.doi.org/10.1158/1078-0432.CCR-12-2426
39. Pardoll DM. The blockade of immune checkpoints in cancer immunotherapy. Nat Rev Cancer 2012; 12:252-64; PMID:22437870; http://dx.doi.org/10.1038/nrc3239
40. Kohrt HE, Houot R, Goldstein MJ, Weiskopf K, Alizadeh AA, Brody J, Müller A, Pachynski R, Czerwinski D, Coutre S, et al. CD137 stimulation enhances the antilymphoma activity of anti-CD20 antibodies. Blood 2011; 117:2423-32; PMID:21193697; http://dx.doi.org/10.1182/blood-2010-08-301945
41. Kohrt HE, Houot R, Weiskopf K, Goldstein MJ, Scheeren F, Czerwinski D, Colevas AD, Weng WK, Clarke MF, Carlson RW, et al. Stimulation of natural killer cells with a CD137-specific antibody enhances trastuzumab efficacy in xenotransplant models of breast cancer. J Clin Invest 2012; 122:1066-75; PMID:22326955; http://dx.doi.org/10.1172/JCI61226
42. Kohrt HE, Colevas AD, Houot R, Weiskopf K, Goldstein MJ, Lund P, Mueller A, Sagiv-Barfi I, Marabelle A, Lira R, et al. Targeting CD137 enhances the efficacy of cetuximab. J Clin Invest 2014; 124:2668-82; PMID:24837434; http://dx.doi.org/10.1172/JCI73014
43. Takei Y, Takigahira M, Mihara K, Tarumi Y, Yanagihara K. The metastasis-associated microRNA miR-516a-3p is a novel therapeutic target for inhibiting peritoneal dissemination of human scirrhous gastric cancer. Cancer Res 2011; 71:1442-53; PMID:21169410; http://dx.doi.org/10.1158/0008-5472.CAN-10-2530
44. Altschul SF, Madden TL, Schäffer AA, Zhang J, Zhang Z, Miller W, Lipman DJ. Gapped BLAST and PSI-BLAST: a new generation of protein database search programs. Nucleic Acids Res 1997; 25:3389-402; PMID:9254694; http://dx.doi.org/10.1093/nar/25.17.3389
45. Bendtsen JD, Nielsen H, von Heijne G, Brunak S. Improved prediction of signal peptides: SignalP 3.0. J Mol Biol 2004; 340:783-95; PMID:15223320; http://dx.doi.org/10.1016/j.jmb.2004.05.028
46. Krogh A, Larsson B, von Heijne G, Sonnhammer EL. Predicting transmembrane protein topology with a hidden Markov model: application to complete genomes. J Mol Biol 2001; 305:567-80; PMID:11152613; http://dx.doi.org/10.1006/jmbi.2000.4315
47. Marchler-Bauer A, Derbyshire MK, Gonzales NR, Lu S, Chitsaz F, Geer LY, Geer RC, He J, Gwadz M, Hurwitz DI, et al. CDD: NCBI's conserved domain database. Nucleic Acids Res 2015; 43:D222-6; PMID:25414356; http://dx.doi.org/10.1093/nar/gku1221